

Small Footprint Multilayered Millimeter-Wave Antennas and Feeding Networks for Multi-Dimensional Scanning and High-Density Integrated Systems

Tarek DJERAFI¹, Nasser GHASSEMI², Olivier KRAMER²,
Bassel YOUZKATLI-EL-KHATIB², Ajay Babu GUNTUPALLI², Ke WU²

¹ INRS-EMT, Montreal, Quebec, Canada H5A 1K6

² Poly-Grames Research Center and Center for Radiofrequency Electronics (CREER) of Quebec, École Polytechnique de Montréal (University of Montreal), Quebec, Canada H3C 3A7

tarek.djerafi@polymtl.ca, ke.wu@polymtl.ca

Abstract. This paper overviews the state-of-the-art of substrate integrated waveguide (SIW) techniques in the design and realization of innovative low-cost, low-profile and low-loss (L3) millimeter-wave antenna elements, feeding networks and arrays for various wireless applications. Novel classes of multilayered antenna structures and systems are proposed and studied to exploit the vertical dimension of planar structures to overcome certain limitations in standard two-dimensional (2-D) topologies. The developed structures are based on two techniques, namely multi-layer stacked structures and E-plane corners. Different E-plane structures realized with SIW waveguide are presented, thereby demonstrating the potential of the proposed techniques as in multi-polarization antenna feeding. An array of 128 elements shows low SLL and height gain with just 200 g of the total weight. Two versions of 2-D scanning multi-beam are presented, which effectively combine frequency scanning with beam forming networks. Adding the benefits of wide band performance to the multilayer structure, two bi-layer structures are investigated. Different stacked antennas and arrays are demonstrated to optimize the targeted antenna performances in the smallest footprint possible. These structures meet the requirement for developing inexpensive compact millimeter-wave antennas and antenna systems. Different structures and architectures are theoretically and experimentally studied and discussed for specific space- and ground-based applications. Practical issues such as high-density integration and high-volume manufacturability are also addressed.

Keywords

Beamforming, corner, horn millimeter-wave antenna and array, multi-dimensional scanning, patch, six-port, slot, Substrate Integrated Waveguide (SIW), Yagi.

1. Introduction

The radio-frequency range from 30 to 300 GHz is defined as millimeter-waves or extremely high-frequency waves. This frequency range provides diversified advantages, depending on specific applications. To name a few, radiation penetrates many common barrier materials, thus enabling concealed objects to be seen [1], the bandwidth is increased which can enhance the spatial resolution for imaging, wireless localization and data rate in communication system [2]-[3]. Short-range and frequency-reusable wireless communication systems have gained enormous importance in the last years such as at 60 GHz which has been recognized as the most attenuated band with its atmospheric absorption. Recently, emerging applications and renewed interests are being reported such as imaging sensors for security and biomedical applications as in [4] and [5] and E-band back-haul interconnectivity for next generation wireless high-throughput cellular base-stations.

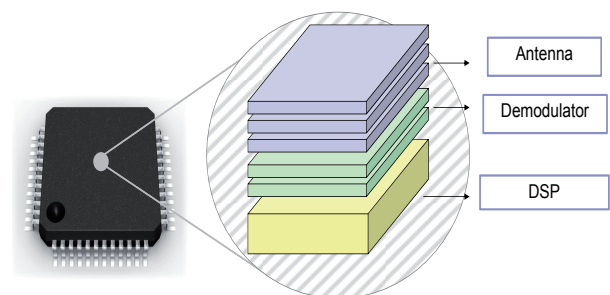


Fig. 1. Illustrative description of a high-density integrated device for millimetre-wave applications.

To enable a widespread acceptance of millimeter-wave circuits and systems in commercial markets, high-density and mass-producible integration techniques need to be developed with low cost. These techniques should deal with challenging issues in the design and development of

the RF front-end and baseband components (Fig. 1). High-gain, high-efficiency, and potentially multi-beam scheme are essential for system cost reduction because the power budget is usually expensive and difficult to meet in practice over such frequency ranges. Such large antenna arrays should also incorporate devices and circuits in connection with associated feed network. Furthermore, various discontinuities within a large feed network should be avoided or used with caution since noise emitted or interference created alters or deteriorates the radiation performance. This is a well-known problem for commonly used planar microstrip, coplanar waveguide or other unbounded planar systems [6]. However, Substrate Integrated Waveguide (SIW) satisfies the foremost part of described constraints.

SIW structures preserve most of the advantages of conventional metallic waveguides, namely high quality-factor and high power-handling capability with self-consistent electrical and mechanical shielding [7-9]. The most significant advantage of SIW technology is the possibility to integrate all the components on the same substrate, including passive components, active elements, and even antenna. SIW circuits can be easily produced with various techniques such as laser drilling, photo-imageable process or other similar processing techniques to satisfy the demand of a more fabrication precision over the millimeter-wave frequency range [10]. Different antenna feeds and beamforming networks (BFN's) have been extensively studied and demonstrated with the SIW schemes and promising results have been obtained [11-16].

Since a number of years, different concepts have been proposed, studied and developed using the third dimension (the vertical dimension) of planar structures to overcome the bottleneck problem of gain, size and footprint within the planar structures. In the following, we will present and discuss various types of antenna arrays and feeding components including innovative feeding mechanisms made of SIW structures. The developed structures are based on two techniques: multi-layer structure and E-plane corner. Since the multi-layer based components are well known, we will just highlight the H-to-E interconnects in the first section. Different antennas, antenna feeds, beam forming networks and components realized in stacked structure or with E corner are detailed. Those schemes show their great flexibility and design capability for low-cost and high-density millimeter-wave applications. Structure designs and prototype results for various applications will be examined. A different design option for future development is discussed.

2. SIW E-plane Components

Bends are essential components in microwave systems. They can be built over H-plane or E-plane and are considered simple components in the standard waveguide technology. However, it seems critical to adopt the designs in new technologies such as SIW in the E-plane. The E-

plane corner is very useful in multi-polarization antenna feeding or to layer-to-layer coupling or feed-through in systems. In this section, two H-to-E interconnect versions in SIW technology are presented.

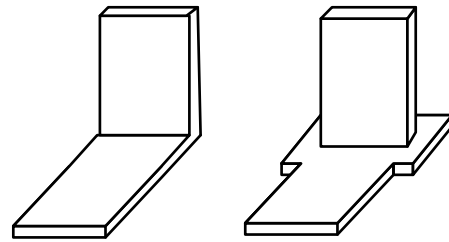


Fig. 2. H-to- E-plane interconnects: a) standard corner bend (type1), b) corner with cavity (type2).

2.1 H-to-E Interconnect

The first interconnect is a real corner, as shown by the TE_{10} wave that continues along the vertical line [17]. To realize the corner, a vertical line is inserted into a horizontal line. A slot was made, having the width of the vertical line substrate thickness and the length equal to the vertical line equivalent waveguide width. The vertical line is terminated by a non-metalized section having the width of the equivalent waveguide and the length equal to the horizontal line substrate thickness. The vertical and horizontal layers making up the corner were fabricated using a conventional printed circuit board (PCB) process, before manually introducing the vertical layer in the horizontal one.

In the second version, the vertical guide is placed at the middle of a cavity in the end of feeding guide [18]. Hence, the maximum power is coupled to the H-plane guide. The cavity's length determines the operating frequency range of the transition. Its width must stay below a certain limit in order to avoid the excitation of parasitic TE_{30} mode, whereas the TE_{20} mode is not critical because of the symmetry of the structure. The photograph of the prototype is illustrated in Fig. 6. The measured bandwidth (return loss ≤ -15 dB) of 11.9% covers frequency band from 71 GHz to 80 GHz. The measured insertion loss is ≤ -2.3 dB over the entire bandwidth. The conductor, dielectric and leakage losses of the SIW add 1.5 dB to the total insertion loss of the transition. The E2H corner has a good agreement between its simulated and measured S-parameters.

	f_0 (GHz)	Bandwidth (%)	Insertion loss dB
Type 1	35	25	0.5
Type 2	77	11.9	1.5

Tab. 1. Performances of the two H-to-E plane interconnects illustrated in Fig. 2

The second version presents the narrowest bandwidth as shown in Tab. 1. In fact, the performance of this struc-

ture depends on the cavity's length. This structure is more robust at higher frequency.

2.2 E-plane T-junction

A simple application of the SIW E-plane corner is related to the design of an E-plane T-junction which presents the function of a transition from one planar SIW structure to another SIW structure perpendicular to the former as well as it acts as a power divider. The junction is constructed by the insertion of a vertical SIW line in the middle of the second line as shown in Fig. 3a. To match the inserted line, two step impedance transformers are used at the corner level. The photograph of a fabricated prototype is shown in Fig. 3b. The 6002 substrate with 0.508 mm of thickness is chosen for this design. The SIW T-junction provides an insertion loss less than 0.5 dB. The measured return loss is better than 10 dB over 19% of the considered bandwidth (31-37.4 GHz) compared to wider than 30 to 38 GHz in the simulated one (23.5%). In addition, the measured phase imbalance of the SIW T-junction is less than ± 4 degree from 32 GHz to 38 GHz.

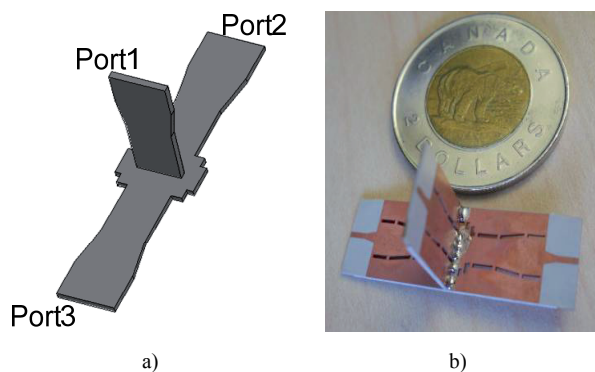


Fig. 3. Topology (a) and photograph (b) of the SIW E-plane T-junction [17].

2.3 E-plane Magic-T

A Magic-T is known as one of the core components in the development of power combiners/dividers, balanced mixers, balanced amplifiers, and feeding networks of antenna arrays. The particularity of the proposed magic-T structure lies in the fact that it represents the first 3D magic-T conventional structure based uniquely on SIW technology without using multilayer technology or slotline-to-SIW transition as in [19]. The proposed structure lies on the design of an H-plane folded magic-T, to which a 180 degree H-plane bend is added in order to redirect the signal to the horizontal plane. The inductive posts are added to ensure low reflection. The 6002 substrate with 0.508 mm of thickness is used in this design. The measured return loss is better than 15 dB for the 30-38 GHz bandwidth at the two input ports. The power splitting is well equalized around 3.5 ± 0.5 dB in the measurement from 31 to 38 GHz. The isolation between the sum and difference ports is bet-

ter than 20 dB and 54 dB from 30 to 38 GHz in simulation. The measured in-phase phase imbalance is ± 2.5 degree and the out-of-phase phase imbalance ± 7.5 degree, respectively.

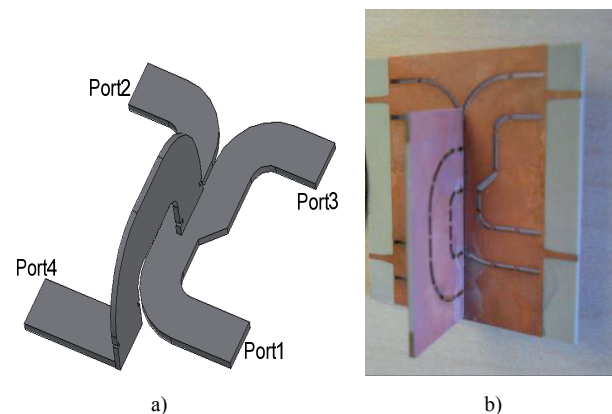


Fig. 4. Topology (a) and photograph (b) of the E-plane SIW magic-T [17].

3. 3-D Millimeter-Wave SIW Antenna and Components

In the following, we will present various types of antenna arrays and feeding networks that show great flexibility and design capability of SIW for low-cost, low-profile, low-loss (L3) and high-density millimeter-wave applications. To simplify our presentations and discussions, selected and representative results are shown to highlight interesting features and attractive performances of those new antenna techniques for millimeter-wave applications.

3.1 Fermi Tapered Slot Antenna Array for Imaging Applications

The antenna architecture for imaging applications should satisfy pre-defined conditions in term of high gain and low side lobe level (SLL). In addition, low cost and light weight characteristics are always required for highly integrated, reliable and portable systems. In fact, those systems are generally duplicated to achieve better resolution, which increase the structure weight and total volume. The proposed design takes into account all those constraints.

The Villeneuve distribution is used for sidelobe reduction [20]. This scheme is developed for the design of Taylor linear arrays when the number of elements is too small for the sampling of a continuous Taylor distribution, generally achieving better results in term of efficiency. Fig. 5a shows one 1/16 power divider and one 4-stage H-plane SIW power divider that make use of equal and unequal-split T-junction power dividers to achieve the required aperture distribution. H-plane bends are used to compensate different delays generated by the imbalanced power splitting arrangement [21]. The equal power divi-

sion in the 4th stage of the power divider represents a compromise that is needed due to the tight dimensions dictated by the element spacing. This modification preserves the 3 dB beamwidth at same value and degrades the SLL. All transmission coefficients fluctuate around the ideal coupling factor in the band of 30 to 40 GHz. With reference to the magnitude, the errors are 5%, 4.56%, 13.13% and 23.71% respectively. Similar to the previous 1/16 power divider, an 8-way T-junction power divider (Fig. 5b) is designed in order to accommodate the feeding for eight samples of the above-discussed 1x16 linear array, thus forming the proposed integrated 8x16 planar antenna array.

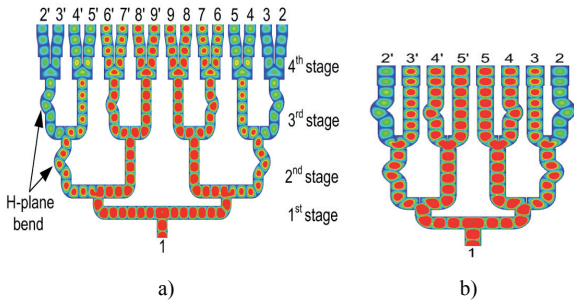


Fig. 5. Simulated E-field magnitude distribution obtained by HFSS at 35 GHz, along the unequally distributed 1/16 and 1/8 principal power dividers [24].

End fire element is chosen to ensure initial high gain and broadband characteristics for the array. Fermi-TSA (tapered slot antenna) structure is used as element to reduce the beamwidth [22]. Corrugation is introduced to reduce the resulting antenna physical width without degradation of performance [23]. At 35 GHz, the simulated gain is about 19.4 dBi and 18.4 dBi is obtained in measurement. The mutual coupling between the elements of antenna arrays must be taken into account during the design process. The previously described antenna topology has been studied to evaluate the isolation levels between two adjacent elements along their E-plane. The isolation is about 13 dB between the elements aligned and separated by $0.68 \lambda_0$. The dielectric is subtracted in the central region and the isolation between the two elements is 3 dB lower. To explain this improvement, simulated E-field distributions are shown in Fig. 6 along the antipodal Fermi-TSA structures with and without the substrate removal. In the modified antenna, the

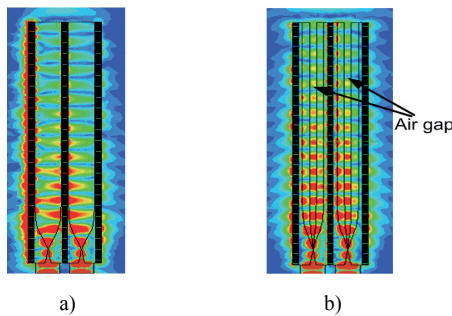


Fig. 6. Simulated E-field magnitude distribution obtained by HFSS along two Fermi-TSA elements at 35 GHz: (a) without the substrate removal, and (b) with the substrate removal [24].

field is more spread along the transverse section. In fact, the air gap creates discontinuities and the field is confined along the air gap. The air slotted version gives more than 1 dB gain improvements. The gain of one simulated Fermi-TSA element in the presence of a second passive element is 2 dB lower than that of a single element. The coupling is very small between two elements disposed in the parallel arrangement.

Fig. 7a illustrates this novel planar array composed of 8x16 antenna elements of corrugated antipodal Fermi-TSA, and fed with an SIW power divider [24]. A 45-degree rotated E-to-H-plane interconnect ensures, with eight 1x16 and one 1x8 power dividers, the construction of one block feeding network for 128 antenna element array [24]. The whole antenna is fabricated with standard PCB process. The gain of the planar array is 27 dBi, and the SLL is better than 26 dB in both E-plane and H-plane as shown in Fig. 7b, the beamwidth is about 5.15 degrees in the E-plane and 6.20 degrees in the H-plane. The total weight of the array is less than 200 g, showing an important advantage of SIW technology in payload efficiency for space and airborne applications. The next step is the integration of phase shifters and distributed amplifiers into the SIW feeding lines to ensure agility and functionality of the antenna systems.

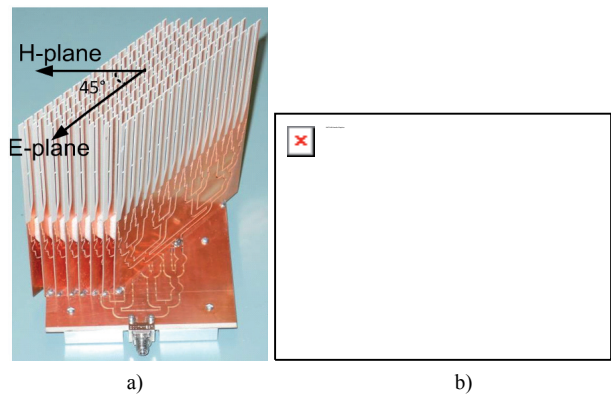


Fig. 7. (a) Photograph of the proposed three-dimensional architecture of 128 element antenna array, (b) E-plane and H-plane radiation pattern performances of the 8x16 SIW corrugated Fermi-TSA planar array at 35 GHz [24].

3.2 2-D Scan Multi-Beam Antenna

The phase control of the array of one dimensional (1-D) frequency scanning arrays is realized by using microstrip Rotman lens in [25] and SIW parabolic reflector in [25], to alleviate the radiation loss of the former microstrip design. The planar array is fed by using multiple R lenses in [26], where the azimuth scanning is obtained by feeding each input of the vertically placed lens. However, such a complex architecture is not suitable for cost effective planar integration. Furthermore, all the cited published topologies occupy large space, and they are not suitable for feeding conformal arrays, where 360° scan coverage is essential.

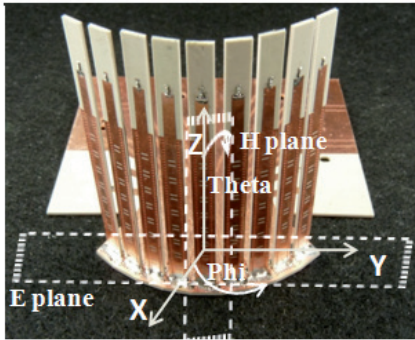


Fig. 8. Fabricated SIW 2-D multibeam antenna, the E plane and H plane are defined with reference to the radiating element [18].

The 2-D scan antenna proposed in [18] is currently under review and further development. Only one of the final prototypes is given here for information. One port leaky-wave antenna (LWA), steering from backward to forward directions including the broad side, is studied and implemented in the SIW technology. The azimuth plane scanning of multi-beam antenna (MBA) is obtained through the phase control of array of nine 1-D elevation plane frequency scanning LWAs, each fed through the vertical corner on the array port contour of the Rotman lens. The complete antenna prototype fabricated on single Rogers RT/Duriod 6002 substrate with $\epsilon_r = 2.94$ and 0.508 mm thickness is simulated through Ansoft HFSS. The periodic frequency scanning antenna has poor radiation efficiency because of the existence of an open stop-band around broad side in the narrow frequency band. In this work, SIW LWA using the concept of reflection cancellation is developed. Directional pattern characteristics are studied and demonstrated from -37° to $+18^\circ$ by changing frequency from 58 GHz to 78 GHz at an interval of 1 GHz. A matched termination is designed, validated and integrated to realize single port LWA.

A 2-D scanning multi-beam conformal array is realized by utilizing Rotman lens BFN feeding nine leaky-wave wave antennas (LWAs) in the azimuth plane for E-plane steering and natural frequency scanning property of 1x8 LWA for H-plane steering. The whole 3-D circuit is constructed after fabricating nine LWAs and then inserted into the slots made on the Rotman lens BFN. The antenna array has seven inputs for beam switching, four dummy ports for sidewall absorption and nine LWAs on the contour of the Rotman lens. The lens is synthesized to distribute the desired amplitude to the radiating elements located on the output ports of the Rotman lens contour.

The experimental results are shown in Fig. 9. The 2-D scanning capability of this multi-beam antenna by covering an azimuth angle of 71.8° (by changing the phase distribution i.e. by changing the input ports 1-7 over 6.6% of array bandwidth at 74.5 GHz) and an elevation angle of 13.5° (by changing frequency from 73 to 78 GHz at each port) in the cross plane. The wideband matching condition (28.5% of 2:1 VSWR bandwidth) is achieved at 70 GHz for the LWA. The multi-beam antenna can efficiently cover the

solid angle of $(49^\circ, 84.5^\circ)$ to $(120^\circ, 70^\circ)$ ((phi, theta)) by multiple beams. Due to its attractive advantages, the proposed MBA is suitable for various scanning applications such as automotive radar and RF switchable software-defined radio. An inexpensive wideband matched termination with satisfactory performance is integrated for sidewalls and also for LWA. This makes the antenna system readily usable; particularly for E-band low-cost commercial car radar applications. The power reaching the output port of the LWA can easily be minimized by just increasing the number of slots without increasing the size of the MBA, for which the vertical dimension can be explored.

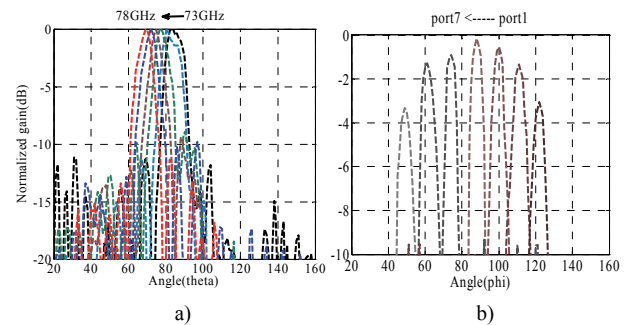


Fig. 9. (a) Measured H-plane patterns excited at Input port 4 versus frequency. (b) Measured E-plane patterns excited from ports 1-7 at 75 GHz.

The multi-dimensional scanning phased array systems have numerous applications in today's wireless and satellite communications for sending and receiving power simultaneously in a multi-user environment. The traditional design of a phased array system consists of power dividers/combiners and phase shifters, which were implemented in standard waveguide technology. The cost and weight of such a phased array system makes practically unsuitable for today's fully integrated system on substrate implementation. The proposed corner can also be used to implement multi-dimensional scan multi-beam antenna as described in [27]. All the efficient phased array system is designed on low loss substrate and fabricated in SIW technology.

3.3 Multilayer Butler Matrix

In the systems employing switched beam antennas, the antenna arrays are associated with BFN to produce multiple beams. To reduce the foot print, we can act on one of these two parts. In the latter session, we act on the antenna using the third dimension to conserve the same surface. In this design and the next one, we present bilayered structures. These structures present the height integrity quality, but also present a relatively larger bandwidth than the planar counterparts.

Butler matrices to scan one dimensional (1-D) linear array were only presented in [28]. The Butler matrix has been considered to be the most attractive BFN option due to its ability to form orthogonal beams, its design simplicity and its lossless property and high beam crossover. In

a planar structure, C crossovers are required to form the beam patterns, for $N \times N$ matrix is $\sum_{k=1}^{\log_2(N)} \left[\frac{N}{2} (2^{k-1} - 1) \right]$

When the number of crossovers involved in the implementation of conventional Butler matrices is high, a larger size will be required. For instance, for a matrix having 32 ports, the number of crossovers is 416, which is very large and it could introduce a higher level of transmission loss (typical 1 dB in the described 4x4 Butler matrix design by crossover). For this reason, a configuration free from crossovers becomes attractive. The double-layer structure is constructed in [29] using a combination of hybrids with broad-wall slot coupling and changes of layers at places in connection with the E-plane couplers. The required phase shift is obtained by H-plane coupler inclinations. The change of layers occurs at places for the second couplers stage and no crossing is required on the same layer.

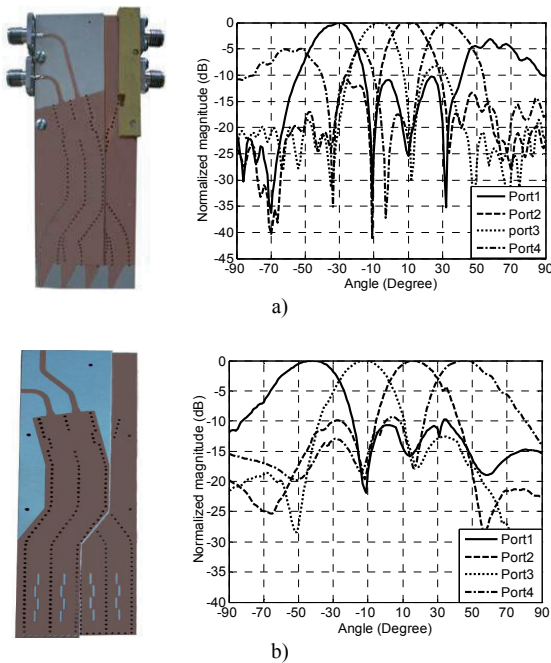


Fig. 10. Photograph and radiation patterns of: a) four ALTSA elements antenna array, b) four slots antenna array, fed by a 4 x 4 Butler matrix made of SIW [29].

The difficulty is the limitation in the fabrication of such double layers PCB, especially for the metalized holes connection to the middle ground of the assembly, and for the air gap between the layers. In fact, 5µm of epoxy with permittivity of 3.5 and 0.03 of loss tangent is used; additional loss and less power equality are observed. The designed matrix has a dimension of 51x28 mm², which is considerably smaller than planar form (about 60% foot print reduction). The simulation of the developed matrix shows excellent performances in the bandwidth of 22 to 26 GHz, with ±1dB power equality, a 0.35 dB of loss in the central frequency and the required phase shift between output ports.

To demonstrate the performance of the proposed matrix, the designed matrix is used to feed a four short end-fire ALTSA antenna. The measured antenna main beam is directed to -32, 10, -10, and 35 degree, respectively, as shown in Fig. 10a. A broadside 4 x 4 array antenna with longitudinal slots etched on the broad wall of the SIW has also been integrated with the proposed matrix, four beams are produced at (-41, -12,-16, 44) degrees as shown in Fig. 10b.

3.4 Multi-layer Six-port Junction

The six-port junction circuit is a passive interferometer device that essentially consists of several couplers, power dividers and one wideband phase shifter (if necessary), and it can be considered as a black box with two inputs and four outputs [30]. Six-port was proposed for the development of low-cost and high-efficient direct-conversion software-defined transceivers and can also use as antenna feed network [31].

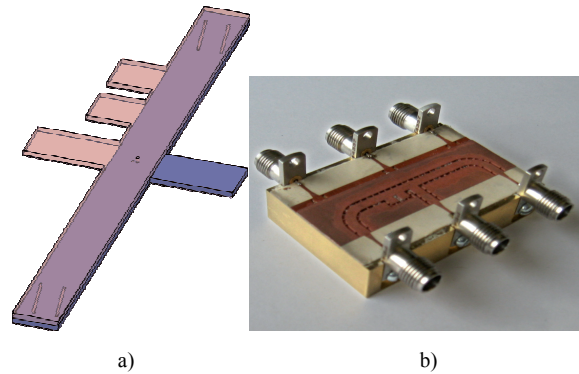


Fig. 11. Bi-layer six-port: a) Topologies of the bilayer structure, b) photograph of the realised prototype with microstrip-SIW transition and V-connectors [32].

A novel dual layered six-port front-end circuit using the SIW technology was presented and demonstrated [32]. The proposed six-port architecture makes use of multilayer couplers, providing a wide coupling area through two slots; a new broadband SIW phase shifter composed of two H-plane stub lines and two SIW power dividers (Fig. 11a). The two-layer coupling structure is very attractive to meet the requirement for low-loss and low-cost as well as high-density integration. The six-port junction was designed with Rogers RT/Duroid 6002 substrate with relative dielectric permittivity of 2.94 and substrate thickness of 0.254 mm. Differences between port-to-port transmission parameters, namely S₃₁ and S₆₁, S₄₂ and S₆₂, S₃₂ and S₅₂, are close to zero. Furthermore, the phase differences between S₃₁ and S₄₁, S₅₁ and S₆₁, S₃₂ and S₄₂, S₆₂ and S₅₂ are close to 90°. The proposed integrated six-port circuit was realized (Fig. 11b) and demonstrates an excellent performance over a large bandwidth. Simulation and measured results show that the proposed six-port circuit can easily operate at 60 GHz for V-band system applications.

3.5 Layer-Stacked Antenna

Multi-layer stacked antennas present the same advantage than the bi-layer junctions presented above, in term of integrality and bandwidth. Four different structures are presented in this subsection.

3.5.1 Yagi-like Array

A novel low-cost, small-footprint and high-gain antenna array is presented for applications over the V-band [33] and W-band [34]. Presented for the first time in [35], the stacked Yagi antennas use the third dimension to control the gain. Designed at 5.8 GHz as the first demonstration prototype, the usual spacing between parasitic elements is quite large and imposes air gaps as the substrate would be too thick to realize. At 60 GHz and higher, with relative substrate permittivity of 2.2 or even higher, the spacing is within the standard processing range, which is in this case, $0.15\lambda_d$ (wavelength in the dielectric) corresponding to a thickness of 0.508 mm.

A single element stacked Yagi antenna fed by microstrip shown in Fig. 12a is studied in order to obtain the desired performance. The radiating element configuration consists of two substrate layers with 0.254 mm of thickness. The circular patch is etched on the top of Layer 2, the feed lines etched on the top of Layer 1 and the ground at its bottom. The spacing is within the standard range which is between 0.15λ and 0.3λ . This standard range was determined in [35] at 5.8 GHz. The gain rises steadily when the number of elements increases up to 8–9 elements, then begins to get saturated as illustrated in Fig. 12b. Compared to the work of Stutzman [36], the antenna gain for the same number of elements is 2.5 dB more in our configuration. The gain drops about 0.2 to 0.5 dB because of the dielectric loss. The measured Yagi antenna attains a gain of 11 dBi over 4.2% of bandwidth with three directors. Yagi antenna is simulated using Ansoft HFSS v12.0.

SIW technology is used to design its feed network. Longitudinal slots in the SIW top metallic surface are used to drive the array antenna elements. A 4×4 array including the one-to-four power divider is realized with SIW technology as shown in Fig. 12c. To avoid the excitation of surface waves, arrays of metallic via holes are placed around the array. The measured results of S-parameters show a 7% bandwidth. A gain of 18 dBi is achieved, which is in good agreement with the simulated results. We observe that the bandwidth increases with the SIW feeding technique compared to the microstrip scheme. The prototyped 4×4 array has a size of 28×24×2.4 mm (including the distributed network feeding). Such a very small footprint technique leads to a far field around 16 cm at 60 GHz that allows a very close scanning unlike standard horn antenna. In [34], the ring shaped director elements are vertically stacked over the circular patch over W-band. To increase the bandwidth of this antenna, the resonant frequencies of the patches and slots are also set to be close to each other. The director elements are etched on low-cost Rogers/Du-

roid 5880 substrate with thickness of $0.12\lambda_d$. This structure shows a gain of 18 dBi.

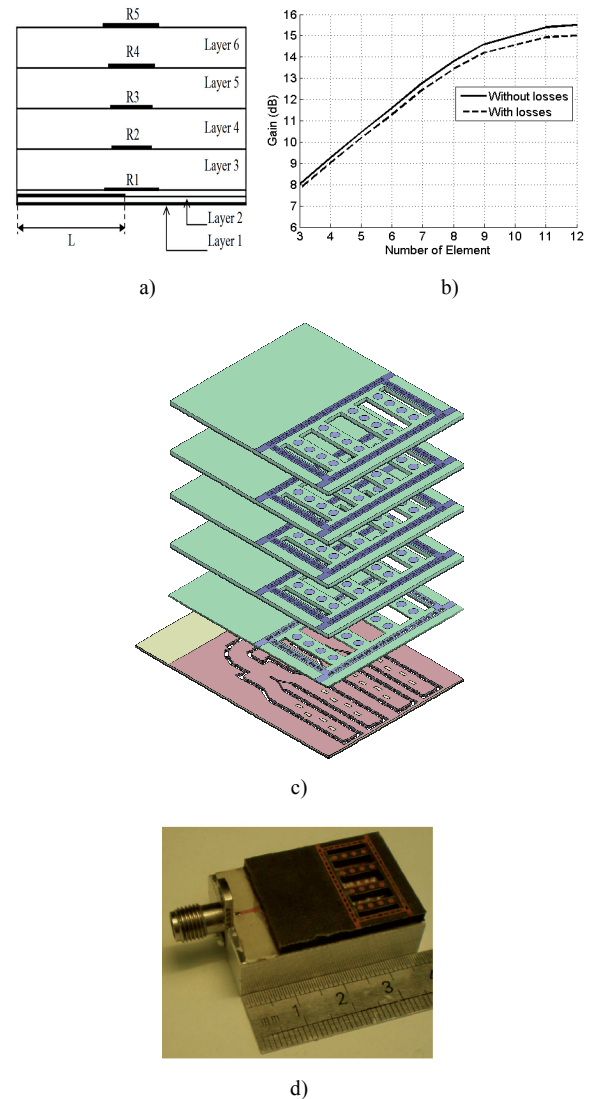


Fig. 12. Vertically stacked Yagi-like antenna array: a) Side view of one patch feed by microstrip line. b) Gain versus number of element. c) Stack-up view of the 4×4 antenna array. d) Photograph of the array [33].

An interesting property of the proposed Yagi antenna is that the directors can control the direction of the main beam. An alternated configuration of the array is studied. It is composed of Yagi elements oriented in different directions with geometrical offset with respect to each other, allowing for a significant 6 dB reduction of SLL in both simulation and measurement.

3.5.2 Broadside Rod Antenna

In [34], the director’s conductors are avoided and the dielectric cube acts as rode. The rod can be rectangular or tapered in one plane or rod is tapered linearly to a point in both the E- and H-planes [37]. Rectangular cubes of low-permittivity material are placed on top of each 1×4 antenna array (Fig. 13a), to increase the gain of the circular patch

antenna elements by 3 dB. Measured impedance bandwidths of the 4×4 antenna array (Fig. 13b) is about 7.5 GHz (94.2-101.8 GHz) at 19 dB measured gain level, with radiation patterns and gains of the array remaining nearly constant over this bandwidth. The measured radiation efficiency of 81 percent is obtained. But the rod structure can be profiled to achieve a better gain.

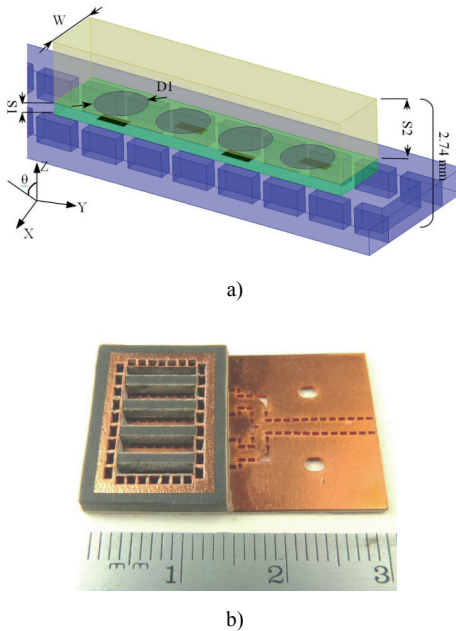


Fig. 13. a) 1x4 antenna array with dielectric cube. b) Photograph of the fabricated 4x4 antenna array with dielectric cubes [34].

Compared with previous millimeter-wave SIW slot antennas, the antenna structures presented in this section result in higher gain, larger bandwidth and higher radiation efficiency with a more stable (less dispersive) gain within the operational bandwidth. The fabrication effort of this array involving dielectric cubes is significantly reduced compared to the 4×4 antenna array which, instead of dielectric cubes, uses vertically stacked Yagi-like parasitic director elements.

3.5.3 Integrated Pyramidal Horn Antenna Made of Low-cost Multilayer Structure

A novel wideband integrated pyramidal horn antennas which can be made of low-cost multilayered structures is presented in [39] for wideband gigabyte point to point wireless applications over E-band (71-76 GHz, 81-86 GHz, and 94.1-97 GHz) [38]. The proposed antenna radiates along the broadside to the substrate. SIW is used to feed the proposed integrated horn antenna. Fig. 14 shows the configuration of a waveguide-based horn antenna and its waveguide feed. On the top metallic surface at the end of SIW, a transverse slot is deployed to drive the horn antenna. To synthesize the horn walls, metallized via holes are used. The horn walls are made of metallic via holes for which the opening of the horn is flared in steps from the second layer to the upper layers. In each layer, the width

and length of the aperture are increased incrementally. Simulation results showed that, increasing the aperture of the antenna (by increasing the number of layer), would increase the gain. A low-cost multilayer standard printed circuit board (PCB) process is utilized to fabricate the proposed multilayer integrated horn antenna on standard Rogers substrate. Measured bandwidth of the antenna is 35 GHz (70-105 GHz) while a relatively constant gain of 10 ± 1 dB is obtained over most of the bandwidth.

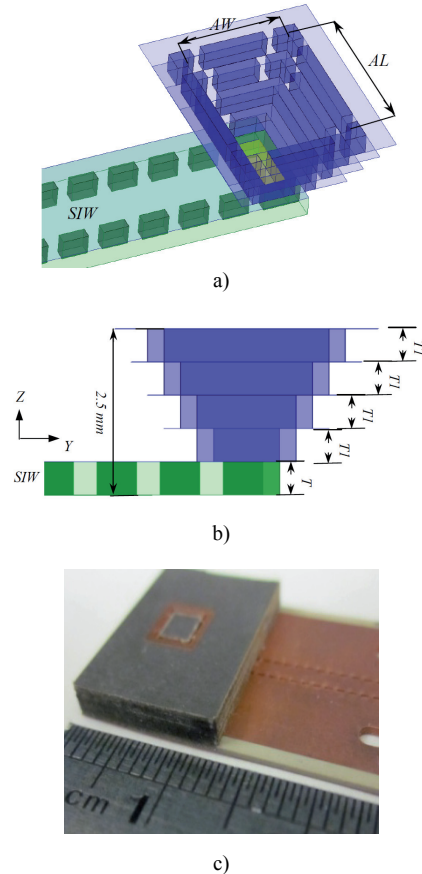


Fig. 14. Structure of a multilayer integrated horn antenna: a) 3D view, b) side view, c) the fabricated antenna [38].

3.5.4 High-efficient Patch Antenna Array for E-band Gigabyte Point-to-Point Wireless Services

A low-cost, high-gain, and high-efficiency 4×4 circular patch array antenna for gigabyte point-to-point wireless services at E-band (81-86 GHz) was presented in [39]. The proposed antenna structure consists of two layers as shown in Fig. 15. The feed network is placed at the bottom layer while the circular patches are on the top layer. The bottom layer is used to support the design of the SIW feeding network and power dividers which are made of a 20 mil Rogers/Duroid 6002 substrate. The top layer which is made of 20 mils Rogers/Duroid 5880LZ substrate involves circular patches that are fed through longitudinal slots etched on the SIW top surface. Low-cost PCB process is again used to fabricate the antenna prototype in two layers.

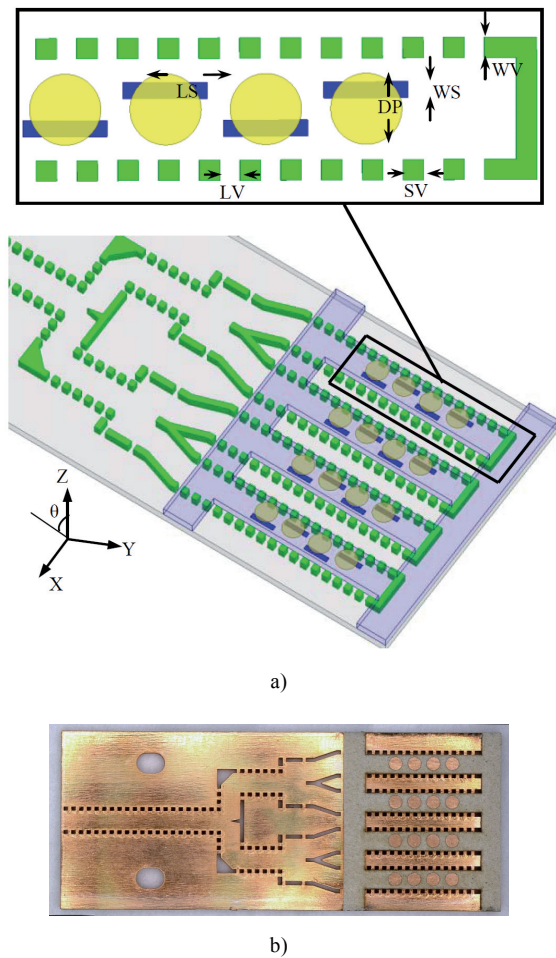


Fig. 15. Geometry, 3-D view and photograph of the fabricated 4x4 antenna array prototype [39].

design	BW (GHz)	Gain (dBi)	thickness (λ_d)
4x4 Yagi-like array 60GHz	58-62	19	0.627
4x4 Yagi-like array 94GHz	94-101	19	0.635
4x4 array with rod	94.2-101.8	19	1.2
Horn	70-105	10	1.17
4x4 Bi-layer array	81 - 86	18.5	0.51

Tab. 2. Comparison between different antennas.

Tab. 2 summarizes the developed multilayer stacked structures. The dimensions of the parasitic elements as well as the spacing between those elements are critical parameters. In fact, the distance is limited by the thickness of available commercial substrates. Compared to the Yagi-like antenna, the number of layers is reduced from six layers to two layers in [39] and the thickness of the antenna is also reduced from 0.627λ to 0.51λ . Compared to the rod array, the thickness of the antenna is reduced from 1.2λ to 0.51λ in the new structure and also the number of layer is reduced from three layers to two layers. To achieve this gain, the distance between the elements was optimized. This optimized structure can be combined with the presented (Yagi, rod) techniques to maintain the gain without increasing the foot print. Bandwidth and radiation efficiency present almost the same order in these structures.

The gain in the different arrays is constant over the bandwidth of interest.

4. Conclusions

A new class of compact and integrated 3-D planar arrays with the benefits of the SIW technology have been proposed, studied, and demonstrated. Four multilayer-stacked arrays have shown a very small footprint with gain and bandwidth improvement. Two multilayered structure are examined (Butler matrix and six port junctions) which can be associated and integrated with the stacked antenna to build very compact transceivers with steerable beam. A planar array, constructed with end-fire antenna ensuring a high gain, is also presented. The proposed architecture is less complex given the fact that vertical and horizontal PCB pieces are easily connected like LEGO blocks. With the integration of phase shifters and distributed amplifiers into the SIW feeding lines, it can be expected that a series of new active array antennas can be developed, which provide a very attractive design alternative for a wide range of microwave and millimeter-wave system applications. Finally, a 2-D scanning multibeam conformal array is realized by utilizing Rotman lens BFN feeding nine LWAs in the perpendicular configuration. The same concept of the LWA associated with end-fire antenna and Butler matrix is used to cover two planes. This work suggests that the proposed concept provides light-weight, low-cost, high performance, and full-integration solutions for imaging and other microwave and millimeter-wave applications.

Acknowledgment

The authors are grateful to several governmental grants agencies for their financial support during this multi-year research work, namely, NSERC of Canada and FQRNT of Quebec. The authors are grateful to S. Dube, J. Gauthier, T. Antonescu, M. Thibault and J. S. Decarie from the Poly-Grames Research Center for their technical supports.

References

- [1] KEMP, M. C. Millimetre wave and terahertz technology for the detection of concealed threats – a review. *Proc. SPIE*, 2006, vol. 6402.
- [2] MEINEL, H. H. Commercial applications of millimeter waves – history, present status and future trends. *IEEE Transactions on Microwave Theory and Techniques*, 1995, p. 1639–1653.
- [3] SCHOEBEL J., HERRERO, P. *Planar Antenna Technology for mm-Wave Automotive Radar, Sensing, and Communications, Radar Technology*. Book edited by: Dr. Guy Kouemou, INTECH, Croatia, December 2009, p. 410.

- [4] GOLDSMITH, P. F., HSIEH, C.-T., HUGUENIN, G. R., KAPITZKY, J., MOORE, E. L. Focal plane imaging systems for millimeter wavelengths. *IEEE Trans. Microwave Theory and Techniques*, October 1993, vol. 41, p. 1664–1675.
- [5] SALMON, N. A. Scene simulation for passive and active millimetre and sub-millimetre wave imaging for security scanning and medical applications. *SPIE*, 2004, vol. 5619, p. 129-135.
- [6] HALL, P. S., HALL, C. M. Coplanar corporate feed effects in microstrip patch array design. *Proc. Inst. Elect. Eng.*, June 1988, vol. 135, p.180–186.
- [7] WU, K., DESLANDES, D., CASSIVI, Y. The substrate integrated circuits – a new concept for high-frequency electronics and optoelectronics. In *6th Int. Conf. on Telecommunications in Modern Satellite, Cable and Broadcasting Service*. Oct. 2003, vol.1, p. 3-5.
- [8] DJERAFI, T., DESLANDES, D., WU, K. A temperature compensation technique for substrate integrated waveguide cavities and filters. *IEEE Transactions on Microwave Theory and Techniques*, Aug. 2012, vol. 60, no. 8, p.2448-2455.
- [9] DJERAFI, T., DESLANDES, D., WU, K. Temperature drift compensation technique for substrate integrated waveguide oscillator. *IEEE Microwave and Wireless Components Letters*, 2012, vol. 22, no. 9, p.489-491.
- [10] DAIGLE, M., DJERAFI, T., WU, K. Modified photoimageable thick-film process for millimeter-wave rectangular waveguide applications. *Progress in Electromagnetics Research C*, 2011, vol. 22, p.137-150.
- [11] LI, Z., WU, K. 24-GHz frequency-modulation continuous-wave radar front-end system-on-substrate. *IEEE Transactions on Microwave Theory and Techniques*, Feb. 2008, vol. 56, p. 278–285.
- [12] CHEN, X.-P., WU, K., HAN, L., HE, F. Low-cost high gain planar antenna array for 60-GHz band applications. *IEEE Transactions on Antennas and Propagation*, June 2010, vol. 58, p. 2126–2129.
- [13] SBARRA, E., MARCACCIOLO, L., GATTI, R. V., SORRENTINO, R. A novel Rotman lens in SIW technology. In *European Radar Conference*, 2007, p. 236-239.
- [14] CHENG, Y. J., HONG, W., WU, K., FAN, Y. Millimeter-wave substrate integrated waveguide long slot leaky-wave antennas and two-dimensional multibeam applications. *IEEE Transactions on Antennas and Propagation*, 2011, vol. 59, no. 1, p. 40-47.
- [15] DJERAFI, T., FONSECA, N. J. G., WU, K. Planar K_u -band 4 4 Nolen matrix in SIW technology. *IEEE Transactions on Microwave Theory and Techniques*, Feb. 2010, vol. 58, no. 2, p. 259–266.
- [16] DJERAFI, T., WU, K. A low-cost wideband 77-GHz planar Butler matrix in SIW technology over. *IEEE Transactions on Antennas and Propagation*, 2012, vol. 60, no. 10, p. 4949-4954.
- [17] YOUZKATLI EL KHATIB, B., DJERAFI, T., WU, K. Substrate integrated waveguide vertical interconnects for three-dimensional integrated circuits. *Transactions on Components, Packaging and Manufacturing Technology*, 2012, vol. 2, no. 9, p. 1526-1535.
- [18] GUNTUPALLI, A. B., DJERAFI, T., WU, K. Integrated waveguide two-dimensional scan conformal multi-beam array antenna. *Transactions on Antennas and Propagation*. Unpublished.
- [19] FENG, W. J., CHE, W. Q., DENG, K. Compact planar magic-T using E-plane substrate integrated waveguide (SIW) power divider and slot-line transition. *IEEE Microw. Wireless Compon. Lett.*, Jun. 2010, vol. 20, no. 6, p. 331–333.
- [20] VILLENEUVE, A. T. Taylor patterns for discrete arrays. *IEEE Transactions on Antennas and Propagation*, 1984, vol. 32, p. 1089–1093.
- [21] ANTHONY, T., ZAGHLOUL, A. I. Designing a 32 element array at 76 GHz with a 33 dB Taylor distribution in waveguide for a radar system. In *IEEE AP-S Int. Symp.*, 2009, p. 1–4.
- [22] SATO, H., SAWAYA, K., WAGATSUMA, Y., MIZUNO, K. Broadband FDTD analysis of Fermi antenna with narrow width substrate. In *IEEE AP-S Int. Symp.*, 2003, vol. 1, p. 261–264.
- [23] DJERAFI, T., WU, K. Corrugated substrate integrated waveguide (SIW) antipodal linearly tapered slot antenna array fed by quasi-triangular power divider. *Progress in Electromagnetics Research C*, 2012, vol. 26, p. 139-151.
- [24] YOUZKATLI EL KHATIB, B., DJERAFI, T., WU, K. Three-dimensional architecture of substrate integrated waveguide feeder for Fermi tapered slot antenna array applications. *IEEE Transactions on Antennas and Propagation*, Oct. 2012, vol. 60, no. 10, p. 4610-4618.
- [25] DONGKYU, L., SANGHYO, L., CHANGYUL, C., YOUNG-WOO, K. A. Two-dimensional beam scanning antenna array using composite right/left handed microstrip leaky-wave antennas. *IEEE/MTT-S Int. Microwave Symposium*, 2007, p. 1883 to 1886.
- [26] SOLE, G. C., SMITH, M. S. Multiple beam forming for planar antenna arrays using a three-dimensional Rotman lens. *IEE Proceedings H Microwaves, Antennas and Propagation*, August 1987, vol. 134, no. 4, p. 375-385.
- [27] GUNTUPALLI, A. B., WU, K. Multi-dimensional scanning multi-beam array antenna fed by integrated waveguide Butler matrix. In *Proceeding of International Microwave Symposium*, 2012, p. 1-3.
- [28] WU, K., CHENG, Y. J., DJERAFI, T., CHEN, X. P., FONSECA, N., HONG, W. Millimeter-wave integrated waveguide antenna arrays and beamforming networks for low-cost satellite and mobile systems. In *European Conference on Antennas and Propagation (EuCAP)*, 2010, p. 1-5, 12-16.
- [29] DJERAFI, T., WU, K. Multi-layered substrate integrated waveguide Butler matrix for millimeter-wave systems. *International Journal of RF and Microwave Computer-Aided Engineering*, May 2012, vol. 22, no. 3, p. 336-344.
- [30] XU, X., BOSISIO, R. G., WU, K. Analysis and implementation of sixport software-defined radio receiver platform. *IEEE Transactions on Microwave Theory and Techniques*, 2006, vol. 54, no. 7, p. 2937–2943.
- [31] DJERAFI, T., DAIGLE, M., BOUTAYEB, H., WU, K. SIW six port circuits for mm-wave radar and radio systems. In *EUMC 2009. Rome (Italy)*, 2009, p. 77-80.
- [32] KRAMER, O., WU, K., DJERAFI, T. Dual-layered substrate integrated waveguide six-port with wideband double stub phase shifter. *IET Microwaves, Antennas & Propagation*, accepted.
- [33] KRAMER, O., DJERAFI, T., WU, K. Very small footprint 60 GHz stacked Yagi antenna array. *IEEE Transactions on Antennas and Propagation*, 2011, vol. 59, no. 9, p. 1022-1030.
- [34] GHASSEMI, N., WU, K., CLAUDE, S., ZHANG, X., BORNEMANN, J. Low-cost and high-efficient W-band substrate integrated waveguide antenna array made of printed circuit board process. *IEEE Transactions on Antennas and Propagation*, 2012, vol. 60, no. 3, p. 1648-1653.
- [35] KRAMER, O., DJERAFI, T., WU, K. Vertically multilayer-stacked Yagi antenna with single and dual polarizations. *IEEE Transactions on Antennas and Propagation*, Apr. 2010, vol. 58, p. 1022-1030.
- [36] STUTZMAN, W. L., THIELE, G. A. *Antenna Theory and Design*. 2nd ed. New York: Wiley, 1998.
- [37] LIOUBTCHENKO, D. V., DUDOROV, S. N., MALLAT, J. A., RÄISÄNEN, A. V. Dielectric rod waveguide antenna for W band

with good input match. *IEEE Microwave and Wireless Components Letters*, 2005, vol. 15, no. 1, p. 4-6.

- [38] GHASSEMI, N., WU, K. W band low cost integrated pyramidal horn antenna made of multilayer printed circuit board process. *IEEE Transactions on Antennas and Propagation*, Sep. 2012, vol. 60, no. 9, p.1-6.
- [39] GHASSEMI, N., WU, K. High efficient array of patch antennas for gigabyte point to point wireless services at E Band. Accepted in *IEEE Antennas and Wireless Propagation Letters*, 2012, p.1-3.

About Authors

Tarek DJERAFI was born in Constantine, Algeria, in 1975. He received the M.A.Sc. and Ph.D. degrees (with distinction) in Electrical Engineering from the École Polytechnique de Montréal, Montréal, QC, Canada, in 2005 and 2011, respectively. He has been with SCP Science Montréal-Canada, as an electromagnetic compatibility (EMC) expert. He is currently a Post-Doctoral Fellow with (INRS-EMT) Montréal, QC, Canada.

Nasser GHASSEMI (SM'10) is working towards his Ph.D. degree in Electrical Engineering at Poly-Grames Research Center, Ecole Polytechnique, Canada, since January 2010. His research interests are in the design of millimeter wave antenna, passive and active components, front-end, and transceiver, for gigabyte wireless communication at E band. He has authored over 12 journal and 9 conference papers.

Olivier KRAMER was born in Lyon, France, in 1984. He received the B.Sc. degree (with distinction) from the ESISAR-INPG, Grenoble France, in 2007 and the M.A.Sc. degree in Electrical Engineering (with distinction) from Ecole Polytechnique, Montreal, QC, Canada in 2010. His current interests involve millimeter-wave multilayer structures.

Bassel YOUZKATLI EL KHATIB received the B.Sc. degree from the (INPT-ENSEEIH), France, in 2008 and the M.A.Sc. degree in Electrical Engineering (with distinction) from Ecole Polytechnique, Montreal, QC, Canada in 2011. His current interests involve millimeter-wave three-dimensional compact integrated structures, antenna arrays, antenna feed chains and RF components design.

Ajay Babu GUNTUPALLI (S'09) received M.TECH (with distinction) from IIT, Kharagpur, India in 2009. He was the recipient of best M.Tech project award in 2009 from IITKGP. He is currently working toward the Ph.D. degree at the École Polytechnique of Montréal, Canada. His current research interests include multi-dimensional scan phased array systems, millimeter wave passive filters, couplers, high performance antenna.

Ke WU is Canada Research Chair Professor in RF and millimeter-wave engineering at Ecole Polytechnique (University of Montreal). He has been Director of Poly-Grames Research Center and Founding Director of Center for Radiofrequency Electronics Research (CREER) of Quebec. He has authored over 860 referred papers, and also books/book chapters and patents. He has held key positions in and has served on various panels and international committees including the chair of many committees and international conferences/symposia including the General Chair of IEEE IMS2012. He has served on the editorial/review boards of many journals, transactions and letters including associate editor, editor and guest editor. He is an elected IEEE MTT-S AdCom member for 2006-2015 and served as chair of the IEEE MTT-S Member and Geographic Activities (MGA) Committee. He was the recipient of many awards and prizes. He is Fellow of the IEEE, Fellow of the Canadian Academy of Engineering and Fellow of the Royal Society of Canada. He was a MTT-S Distinguished Microwave Lecturer.